Clinical Biomechanics 68 (2019) 151–157

Contents lists available at ScienceDirect

Clinical Biomechanics

journal homepage: www.elsevier.com/locate/clinbiomech

Intraoperative experiments combined with gait analyses indicate that active state rather than passive dominates the spastic gracilis muscle's joint movement limiting effect in cerebral palsy

Cemre S. Kaya[a], Fuat Bilgili[b], N. Ekin Akalan[b,c], Yener Temelli[b], Filiz Ateş[a,d], Can A. Yucesoy[a,*]

[a] Institute of Biomedical Engineering, Boğaziçi University, Istanbul, Turkey
[b] Istanbul Faculty of Medicine, Department of Orthopaedics and Traumatology, Istanbul University, Istanbul, Turkey
[c] Faculty of Health Sciences, Department of Physiotherapy and Rehabilitation, Istanbul Kültür University, Istanbul, Turkey
[d] Motion Analysis Laboratory, Department of Orthopedic Surgery, Mayo Clinic, Rochester, MN, USA

ARTICLE INFO

Keywords:
Cerebral palsy
Spastic muscle
Gait analysis
Muscle force-knee angle characteristics
Intermuscular mechanical interactions
Epimuscular myofascial force transmission

ABSTRACT

Background: In cerebral palsy, spastic muscle's passive forces are considered to be high but have not been assessed directly. Although activated spastic muscle's force-joint angle relations were studied, this was independent of gait relevant joint positions. The aim was to test the following hypotheses intraoperatively: (i) spastic gracilis passive forces are high even in flexed knee positions, (ii) its active state forces attain high amplitudes within the gait relevant knee angle range, and (iii) increase with added activations of other muscles.
Methods: Isometric forces (seven children with cerebral palsy, gross motor function classification score = II) were measured during surgery from knee flexion to full extension, at hip angles of 45° and 20° and in four conditions: (I) passive state, after gracilis was stimulated (II) alone, (III) simultaneously with its synergists, and (IV) also with an antagonist.
Findings: Directly measured peak passive force of spastic gracilis was only a certain fraction of the peak active state forces (maximally 26%) measured in condition II. Conditions III and IV caused gracilis forces to increase (for hip angle = 45°, by 32.8% and 71.9%, and for hip angle = 20°, by 24.5% and 45.1%, respectively). Gait analyses indicated that intraoperative data for knee angles 61–17° and 33–0° (for hip angles 45° and 20°, respectively) are particularly relevant, where active state force approximates its peak values.
Interpretation: Active state muscular mechanics, rather than passive, of spastic gracilis present a capacity to limit joint movement. The findings can be highly relevant for diagnosis and orthopaedic surgery in individuals with cerebral palsy.

1. Introduction

In individuals with spastic cerebral palsy (CP), the mechanism of pathological resistance against joint extension is unknown. This is ascribed to the passive and active properties of spastic muscles. Regarding the former, the range of joint motion can be limited even in the absence of any active force exertion (Farmer and James, 2001; Fergusson et al., 2007). Therefore, passive forces of spastic muscles are expected to be high (Shortland et al., 2002). In contrast, in the upper extremity, intraoperative measurements revealed low passive forces for spastic flexor carpi ulnaris muscle (Kreulen and Smeulders, 2008; Smeulders et al., 2004). However, in the lower extremity, this has not been measured directly, whereas assessments using muscle biopsies (e.g., Smith et al., 2011), and dynamometry and ultrasound shear wave elastography (e.g., Haberfehlner et al., 2015) demonstrated greater passive muscle stiffness in children with CP compared to typically developing (TD).

Regarding active properties, the role of spasticity in disrupting voluntary active motion has been supported (Crenna, 1998; Damiano et al., 2006) or rejected (Ada et al., 1998; Norton et al., 1975) by various studies. However, the pathological restricted joint motion of CP patients is clear. In the upper extremity, if the limb is pulled on, the joint is forcefully kept in a flexed position (Van Heest et al., 1999), indicating the presence of high flexor forces, which can stem from active force production of spastic muscles. Intra-operative tests allow for the quantification of human muscles' forces directly as a function of joint angle (Yucesoy et al., 2010) and measure their capacity to affect joint moments. A series of studies in patients with CP showed that

* Corresponding author at: Institute of Biomedical Engineering, Boğaziçi University, 34684 Çengelköy, Istanbul, Turkey.
E-mail address: can.yucesoy@boun.edu.tr (C.A. Yucesoy).

https://doi.org/10.1016/j.clinbiomech.2019.06.005
Received 21 March 2019; Accepted 4 June 2019
0268-0033/

activated spastic knee flexors, the gracilis (GRA), semitendinosus (ST) and semimembranosus (SM) muscles, produce only low forces in flexed knee positions (Ates et al., 2013b, 2016; Yucesoy et al., 2017). Note however that, if another muscle is co-activated, spastic GRA muscle's overall mechanical characteristics were shown to change, with the peak force shifting to flexed knee positions for some patients (Ates et al., 2014). This was ascribed to intermuscular mechanical interactions. This through epimuscular myofascial force transmission (EMFT) (Yucesoy, 2010) have been shown to change the force of a muscle explained by its altered force production due to manipulated sarcomere lengths (Maas et al., 2003). Daily activities involve the simultaneous activation of several muscles (Arnold et al., 2007). Therefore, intermuscular mechanical interactions can affect active state mechanics of spastic muscle in CP.

Despite the contribution of previous studies, there are major gaps in our understanding of the passive and active state mechanics of spastic muscles. Although spastic muscle's passive forces are considered to be high, they have not been assessed directly. Additionally, activated spastic muscle's force-joint angle relations were studied independent of gait relevant joint positions. The aim was to fill in these gaps by combining intraoperative experiments with gait analyses in order to test the following hypotheses: (i) spastic GRA passive forces are high even in flexed knee positions, (ii) its active state forces attain high amplitudes within the gait relevant knee angle (KA) range, and (iii) increase with added activations of other muscles.

2. Methods

Surgical and experimental procedures, in strict agreement with the guidelines of the Helsinki declaration, were approved by a Committee on Ethics of Human Experimentation at Istanbul University, Istanbul. The patients and/or their parents gave informed consent to the work.

2.1. Participants

Seven patients (all male: mean age 9 years 2 months, range 6–13 years, standard deviation 2 years 10 months) with CP, however no prior remedial surgery, were included. Gross Motor Functional Classification System (GMFCS) levels of all participants were II. Clinical spasticity scores: popliteal angles measured according to Modified Tardieu Scale and Modified Ashworth Scale scores (Table 1). Prior to surgery, computerized gait analysis was performed for an objective diagnostic assessment. Note that, we used this data to build relationship between the specific spastic muscle level joint angle-muscle force measurements and global patient motion characteristics i.e., to judge the spastic muscle's mechanics against the patients' pathological movement. Overall, pre-operative clinical examinations indicated a severely limited knee range of joint motion and led to a decision that all patients required remedial surgery including release of hamstrings and hip adductors.

2.2. Gait analysis

A motion analysis system (ELITE 2002, BTS Bioengineering, Milan, Italy) with six infrared cameras and two force plates (Kistler Instrumente AG, Winterthur, Switzerland) was used implementing Helen Hayes Marker Placement Protocol (Davis et al., 1991). Bilateral marker locations: the metatarsal head V, heel, lateral malleolus, tibial wand, femoral lateral epicondyle, femoral wand, and anterior superior iliac spine (ASIS). A single marker was placed onto the sacrum. Additionally, a marker on the seventh cervical vertebrae (C7) was used to detect initiation of walking, and to quantify shoulder tilt relative to horizontal in combination with two shoulder markers (on the flat portions of the acromion). Hip and knee joint angles and moments in the sagittal plane were used to relate the global gait metrics to intraoperative spastic muscle level mechanics.

2.3. Intraoperative measurements

Six of the patients were operated on bilaterally. For three of them, separate experiments were performed on both legs. For the remainder patients, only one leg was experimented due to time limitations imposed by subsequent multilevel surgery. Therefore, a total of ten knee angle GRA muscle force (KA-F_{GRA}) data sets were collected. The intraoperative measurements were done first in the passive state (condition I), then the spastic GRA was stimulated alone (condition II), simultaneously with its synergists ST and biceps femoris (BF) (condition III), and also with its antagonist rectus femoris (RF) (condition IV).

The patients received general anesthesia without the use of muscle relaxants or tourniquet. All experimental preparations and data collection were performed after routine incisions to reach the distal GRA tendon and before any other routine surgical procedures. Using a scalpel blade (number 18), a longitudinal skin incision was made immediately above the popliteal fossa. After cutting the adipose tissue, the distal GRA tendon was exposed. Subsequently, a buckle force transducer (TEKNOFIL, Turkey) (Fig. 1A) was mounted and fixed over the tendon. The key transducer characteristics include S-shape; dimensions: width = 12 mm length = 20 mm and height = 9 mm; maximal force range = 400 N; for test range 0-200 N: accuracy < 3%, (< 0.19% below 100 N); resolution = 0.62 N and high linearity (R^2 = 0.99963,

Table 1
Patient characteristics and spasticity scores.

Patient	Limb	Age (years)	L_{thigh} (cm)	$C_{mid\text{-}thigh}$ (cm)	PA (°) - R1 of MTS	PA (°) - R2 of MTS	MAS score adductor	MAS score hamstring
1	1	13	36.0	40.5	65	60	1	2
1	2	13	36.5	39.0	70	65	2	2
2	3	8	30.0	32.5	70	50	1+	2
3	4	8	31.0	36.0	75	40	2	2
3	5	8	31.0	35.8	60	50	1+	1+
4	6	6	27.0	29.2	65	65	1+	2
5	7	11	35.0	43.0	80	80	2	2
6	8	12	37.0	37.0	80	80	2	2
6	9	12	38.0	39.5	70	70	1+	2
7	10	6	26.0	28.0	80	65	1+	1+

L_{thigh} = thigh length; $C_{mid\text{-}thigh}$ = mid-thigh circumference; PA, Popliteal angle (i.e., the angle between hip and knee at hip in 90° flexion); MTS, Modified Tardieu Scale; R1 and R2, PA measurements according to MTS per fast and slow-sustained stretch, respectively; MAS, Modified Ashworth Scale.
PA > 50° indicates a severely limited range of knee joint motion.
MAS scores (0, 1, 1+, 2, 3 and 4) other than 0 indicate spasticity. 1: slight increase in muscle tone, manifested by a catch and release or by minimal resistance at the end of the range of motion when the affected part(s) is moved in flexion or extension, 1+: slight increase in muscle tone, manifested by a catch, followed by minimal resistance throughout the remainder (less than half) of the range of movement, 2: more marked increase in muscle tone through most of the range of motion, but affected part(s) easily moved. 3–4 (not present in the current study): for affected part(s), movement is difficult or rigid.

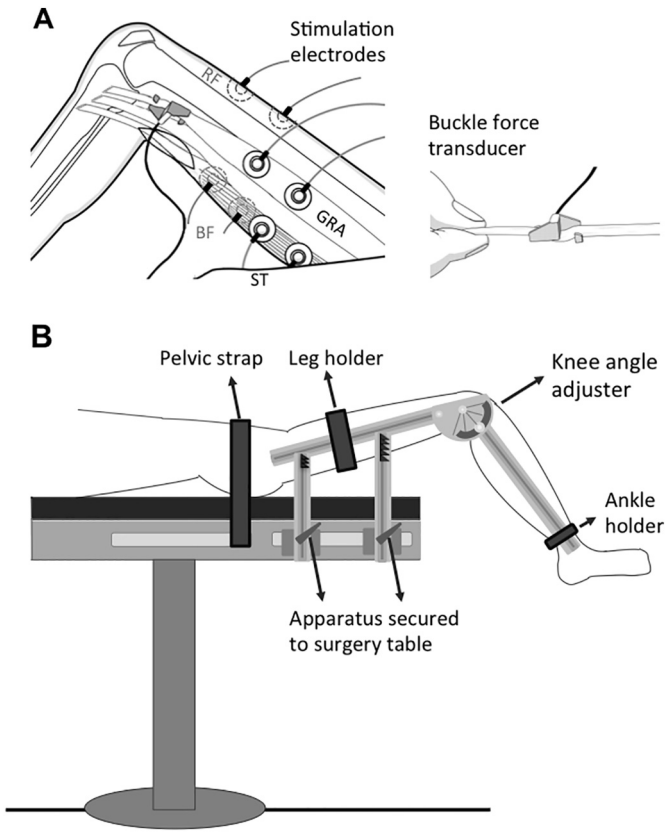

Fig. 1. Buckle force transducer and intraoperative muscle mechanics experimental setups. (A) Illustration of how the buckle force transducer is mounted over target muscle's tendon. Inset shows the transducer mounted over a tendon strip. Pairs of skin electrodes placed over the muscles are illustrated using solid (for the GRA and ST), or dashed (for the long head of BF and RF) circles. (B) An apparatus designed for intraoperative tests in lower extremities is composed of four components: (i) The *upper leg component* incorporating a leg holder, which has an adjustable position on it allows fixing the hip angle (to 45° or 20° both in the sagittal and frontal planes). This component is secured to the slot of the surgery table via fixtures. (ii) The *lower leg component* incorporating an ankle holder that has an adjustable position on it supports the lower leg. (iii) The *knee angle and* (iv) *hip angle adjusters* link together the upper and lower leg components and allows setting the knee and hip angle and fixing them during a contraction. Circular slots were machined in the knee and hip angle adjusters and angles were marked on them (in 0.5° increments) for the required joint position adjustments. The leg holders' position is adjustable on the upper leg component. This allows supporting the upper leg and aligning it such that the axis of the knee and hip joint rotations corresponded to the center of the rotation of the knee and hip angle adjusters, respectively. The ankle holder, position of which is adjustable on the lower leg component allowed supporting the lower leg. The leg holder and ankle holder were sterilized components. The non-sterile remainder parts were covered with sterile fabric before an antiseptic agent was applied to the skin and the patient's leg was positioned and secured to the apparatus.

peak nonlinearity = 1.31%). Note that prior to each experiment, the force transducer was (i) calibrated using bovine tendon strips (with rectangular cross section, dimensions 7 × 2 mm^2 representative of that of the GRA distal tendon) and (ii) sterilized (using gas sterilization at maximally 50 °C).

The patient was positioned, and target joint angles were adjusted using an apparatus (see Fig. 1B for details). Isometric spastic $F_{GRA\_passive}$ and F_{GRA} were measured at various muscle lengths imposed by manipulating the joint angles. Data collection was done in the following sagittal hip and knee angles. The hip position was fixed at two different hip angles (HA) equaling 45° and 20° determined from gait analyses (see Results). For each HA, the KA was manipulated. Note that the hip was positioned in neutral position for ab/adduction and internal/external rotation during testing. Length history effects of previous active contraction of muscle at long length on forces measured at short length (Huijing and Baan, 2001; Yucesoy et al., 2010) were eliminated before acquiring data by preconditioning muscle-tendon complexes and their epimuscular connections. Isometric contractions were alternated at extended and flexed knee positions, until spastic GRA forces at flexed knee position were reproducible. Additionally, the data acquisition was started in a highly flexed knee (120°), and the muscle length was manipulated by extending the knee in 30° increments until 0° (full knee extension). Testing was completed for all conditions before attaining a different knee angle. After each contraction, the muscle was allowed to recover for a minute and completion of the protocol approximated 30 min. A data acquisition system (MP150WS, BIOPAC Systems, CA, USA, 16-bit A/D converter, sampling frequency 40 kHz) was used with an amplifier for the force transducer (DA100C, BIOPAC Systems, CA, USA).

Four pairs of gel-filled skin electrodes (Kendall H92SG, Covidien, MA, USA) were placed on the skin, over the spastic GRA, ST, BF and RF muscle bellies. Muscle bellies were located by palpation. The reference electrodes were placed as distal as possible to the incision with their positions having an offset. The location of the second electrode was determined according to the following procedure: The minimum center-to-center inter-electrode distance was reported to be 30 mm for a successful electrode function (Mathur et al., 2005) and muscle excitation (Gomez-Tames et al., 2012). At KA = 120°, a tentative location for the second electrode was determined accordingly. The contraction responses were assessed in response to twitch stimuli evoked separately for each muscle. Successful stimulation of spastic GRA was monitored from the measured force, and leakage of current into other muscles than the one stimulated was controlled by palpation. This was repeated at, KA = 60° and 0°. If necessary, the second electrode position was optimized by iteration.

A custom made, constant current high voltage source (cccVBioS, TEKNOFIL, Istanbul, Turkey) was used to impose supramaximal muscle stimulation (transcutaneous electrical stimulation with a bipolar rectangular signal, 160 mA, 50 Hz): two twitches were evoked which, after 300 ms, were followed by a pulse train for 1000 ms to induce a tetanic contraction and a subsequent twitch (see Fig. 2 for superimposed examples of force-time traces for spastic GRA muscle at five KAs).

2.4. Processing of data

For each KA tested, $F_{GRA\_passive}$ measured in passive state and F_{GRA} measured in active state, during a 500 ms period (in the middle of the tetanus for F_{GRA}) were averaged and recorded as muscle passive and total force, respectively.

Using a least squares criterion, KA-F_{GRA} data were fitted with a

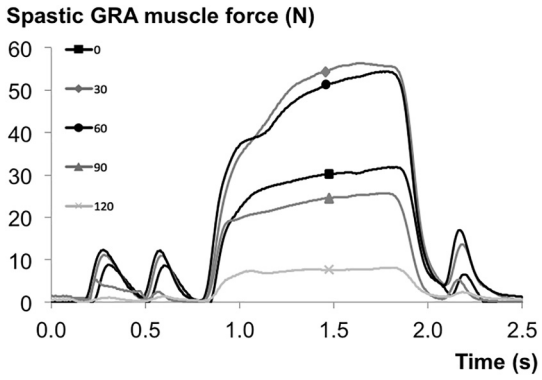

Fig. 2. Typical examples of force-time traces for spastic GRA muscle. Superimposed traces recorded for GRA muscle at the five knee angles studied are shown.

polynomial function

$$F_{ST} = a_0 + a_1KA + a_2KA^2 + ...+a_nKA^n \quad (1)$$

a_0, $a_1 \ldots a_n$ are coefficients determined in the fitting process.

The lowest order of the polynomials and the exponential functions that still added a significant improvement to the description of changes of KA-F_{GRA} were selected using a one-way analysis of variance, ANOVA. KA-$F_{GRA\_passive}$ data were also fitted in the same way. The fitted data for each condition were used to calculate the mean of GRA forces and standard deviations per KA. Range-F_{GRA} (operational KA range of F_{GRA} exertion i.e., range between the KA's at which, the peak and minimum F_{GRA} is measured) was used as an active state metric.

2.5. Statistics

Two-way ANOVA (factors: KA and condition) was used to compare the overall mechanical characteristics of spastic GRA muscle in all conditions. If significant main effects and an interaction were found, Bonferroni post-hoc tests were performed to further locate significant within-factor force differences. Shapiro-Wilk normality test was used to check if the key active state metrics data are normally distributed. Range-F_{GRA} calculated for each limb in Condition III and Condition IV were compared to those of Condition II using paired-*t*-test or Wilcoxon signed-rank test where appropriate. Differences were considered significant at $P < 0.05$.

3. Results

Fig. 3 shows the ensemble-averaged joint angles and moments in the sagittal plane. With less than one SD (for HA 11.1° and KA 8.8°) variation, the following parts of the gait cycle (GC) characterize the pathological joint condition of the patients and indicate gait relevant KA range per HA tested intraoperatively: (i) Exaggerated knee flexion occurs for 0–30% GC and 75–100%. For the patients, this indicates that at the start and end of GC, their knee is highly flexed instead of being typically extended, which compromises heel strike leading even to toe landing. In the gait data, HA = 45° is observed for 0–12% and 77–100% GC, and this matches with KA = 17–61°. (ii) The knee moment is flexor for 16–51% GC instead of being typically extensor, which also agrees with the patients' limited knee extension condition. In the gait data, HA = 20° is observed for 16–37% GC, and this matches with KA = 0–33°. Consequently, intraoperative data for KA = 17–61° at HA = 45° and KA = 0–33° at HA = 20° were determined to represent the pathological movement during loading response/terminal swing, and mid/terminal swing phases of the patients' gait, respectively.

Fig. 4 shows KA-F_{GRA} and KA-$F_{GRA\_passive}$ characteristics. For both HA, in conditions I and II: (1) passive forces start from non-zero, but low amplitudes in flexed knee positions and increase to maximally 26.1% (HA = 20°) of the peak total force measured in condition II. (2) Total forces attain their minimum in the most flexed knee position, show an increases in response to added knee extension, reach a maximum and decrease (for HA = 45°, F_{GRA} = 24.0 N, 70.1 N, 69.2 N at KA = 120°, 16° and 0°, and for HA = 20°, F_{GRA} = 25.8 N, 72.9 N, 67.6 N at KA = 120°, 34° and 0°, respectively).

ANOVA (factors: KA and condition) showed significant main effects of both factors on spastic GRA forces, but no significant interaction. Condition I: the passive forces measured at HA = 20° are significantly (on average by 6.5%) higher than those measured at HA = 45°. Condition II vs. III and IV: co-activation of the synergistic and antagonistic muscles caused spastic GRA total forces to increase significantly (on average, for HA = 45°, by 32.8% and 71.9%, and for HA = 20°, by 24.5% and 45.1% in conditions III and IV, respectively). Compared to HA = 45°, for HA = 20°, the total forces are higher in conditions II and III (on average by 12.9% and 6.1%, respectively) and lower in condition IV (on average by 4.6%). Condition I vs. IV: peak passive force is maximally 18.7% (HA = 20°) of peak GRA total force.

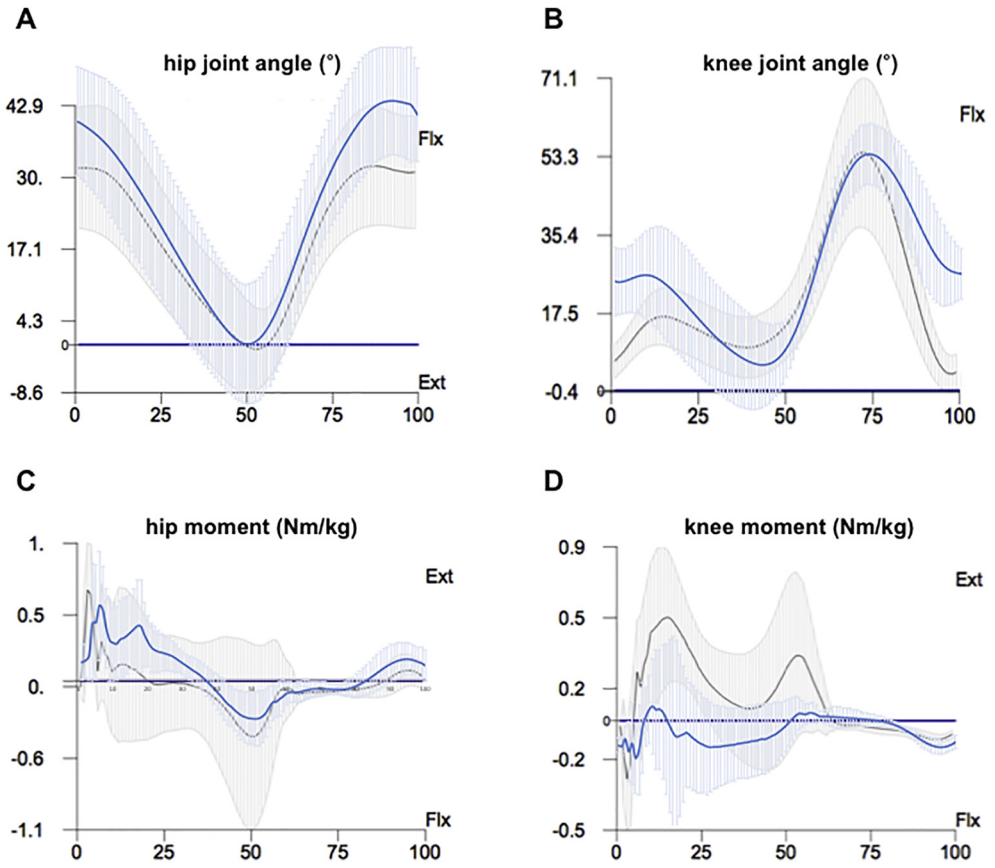

Fig. 3. The patients' gait data. The ensemble-averaged data (A) and (C) for the hip, and (B) and (D) for the knee, showing joint angles and moments, respectively. Blue lines indicate the patients' data, whereas the black lines indicate the reference data for the typically developing children (from the database of the BTS Bioengineering system). Flexion (Flx) and extension (Ext) are indicated. (For interpretation of the references to colour in this figure legend, the reader is referred to the web version of this article.)

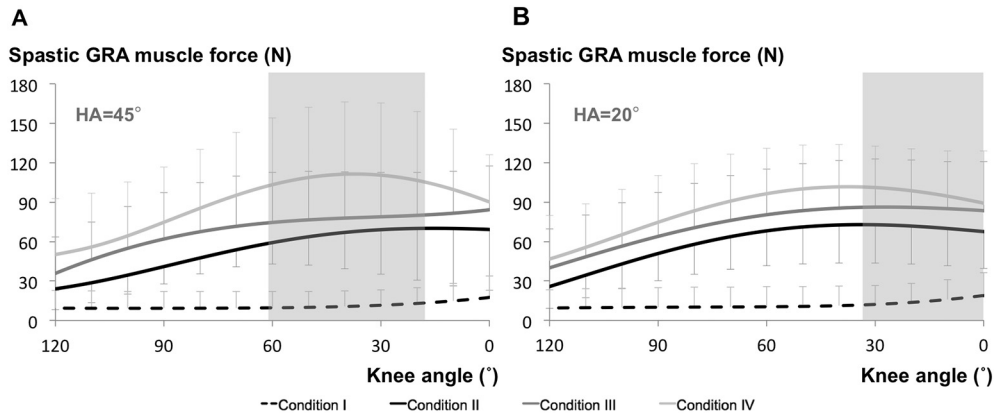

Fig. 4. The mean (SD) of spastic GRA forces of intraoperatively tested limbs per KA across the conditions tested. The spastic GRA forces in the passive states (condition I) are shown as dashed lines. The spastic GRA was activated alone (condition II), simultaneously with its synergists, semitendinosus (ST) and biceps femoris (BF) (condition III), and also with its antagonist rectus femoris (RF) (condition IV). The gray shaded areas show the gait relevant KA-positions.

Table 2
Effects of conditions III and IV on Range-F_{GRA} for each limb tested.

Limb	Range-F_{GRA} (°) for KA = 45°			Range-F_{GRA} (°) for KA = 20°		
	Condition II	Condition III	Condition IV	Condition II	Condition III	Condition IV
1	120	120	90	92	103	94
2	118	120	86	81	95	83
3	77	74	67	60	67	67
4	68	120	63	95	56	82
5	83	120	78	76	88	69
6	120	120	100	92	95	95
7	72	120	120	120	120	120
8	120	98	81	108	92	58
9	120	50	74	73	38	78
10	120	120	97	113	113	88
Mean (SD)	102 (23)	106 (25)	86 (17)	91 (19)	87 (26)	83 (18)

Condition II vs. III and IV: Wilcoxon signed-rank test (conditions III and IV at HA = 45°) and the paired-*t*-test (conditions III and IV at HA = 20°) showed no significant differences in Range-F_{GRA} (Table 2). Across different HAs, no significant differences were shown in Range-F_{GRA} for condition II (Wilcoxon signed-rank test) and condition IV (paired-t-test) but, in condition III, compared to HA = 45°, Range-F_{GRA} was significantly narrower (Wilcoxon signed-rank test) at HA = 20° (on average by 18.1%).

4. Discussion

Passive forces of spastic GRA muscle measured directly at the tendon for the first time maximally approximated a quarter of the active state forces in extended knee positions. Therefore, the hypothesis that spastic GRA passive forces are high even in flexed knee positions was rejected. However, the hypotheses that active state forces of spastic GRA attain high amplitudes within the gait relevant KA range, and increase with added activations of other muscles were confirmed.

The overall mechanical characteristics of spastic GRA in conditions I and II provide valuable novel information as the muscle's passive and active state mechanics can be compared. The fact that the passive state forces are only a certain fraction of the active state forces for most knee positions indicate that the passive state is not the dominant component of the spastic muscle's mechanics affecting the knee joint. This is valid also within the KA range relevant to gait. On the other hand, conditions involving co-activation of other muscles promote testing of the active state effects. Therefore, the intermuscular mechanical interaction effects in conditions III and IV characterize the change in the effects of the active state on the mechanics of spastic GRA. Accordingly, in condition III, elevated forces measured in response to the co-activation of synergistic muscles indicate an increased contribution of spastic GRA to knee flexion moment for gait relevant joint positions due to EMFT. Moreover, further elevated forces of spastic GRA in response to added activation of an antagonist muscle in condition IV strengthen the judgement that the active state dominates the spastic muscle's effect at the joint to cause motion restriction. This is plausible also for other types of daily motions. For self-ambulant children with CP, sit-to-stand and stair ascending/descending involve a KA range approximating 20° to 100° (Lewerenz et al., 2017; Yonetsu et al., 2015) which is within the range of knee positions covered in the current study. Also such key movements involve simultaneous activation of several lower-limb muscles including the GRA, ST, BF and RF (He et al., 2007). Therefore, conceivably EMFT may have similar effects on spastic muscle's mechanics contributing to the restricted joint movement for various types of movements. Note that, sit-to-stand involves further flexed hip positions, which is more pronounced in children with CP compared to TD (Yonetsu et al., 2015). This can cause the GRA to attain shorter lengths proximally and based on the present findings may elevate the effect of EMFT. Hence, plausibly the active state may play a dominant role in limited joint mobility also for sit-to-stand motion. However, these issues require further specific testing.

Notably, (1) in condition IV, GRA forces measured at a HA of 45° were higher compared to those at a HA of 20°. (2) In condition III, Range-F_{GRA} determined for a HA of 20° was significantly narrower than that for a HA of 45°. These findings indicate the effects of epimuscular myofascial loads on mechanics of spastic GRA. Altered HAs change a muscle's relative position with respect to other muscles, which stretches its epimuscular connections and cause myofascial loads to develop (Maas et al., 2003; Yucesoy, 2010). This is the central mechanism for EMFT effects in which such loads can (i) integrate with the muscle's force, or (ii) alter its sarcomere lengths, hence change the muscle's own force and movement production capacity. Regarding the latter, EMFT causes sarcomeres in the same muscle fibers to attain different lengths as well as heterogeneity of mean sarcomere lengths across different fibers (Karakuzu et al., 2017; Pamuk et al., 2016; Yucesoy and Huijing, 2012). A consequence is an altered length range of force exertion

(Yucesoy, 2010; Yucesoy and Huijing, 2009). Additionally, myofascial loads can cause sarcomeres to attain lengths closer to their full myofilament overlap (Huxley and Peachey, 1961; Willems and Huijing, 1994). Both mechanisms can be found in the present data suggesting that the present EMFT effects can be ascribed to both (i) and (ii). Such effects are plausible also for the other findings of the study, however the amplitude and type of effects of epimuscular myofascial loads appear to vary across conditions. Nevertheless, the findings show that such loads did affect spastic GRA muscle's overall mechanics particularly for the gait specific joint positions studied. In order to assess if this reflects on the joint movement limitation, we sought for a correlation between the severity of the patients' pathological gait and the increase in spastic GRA force via co-activation of other muscles (please see the Supplement for details). This assessment indicates that there is indeed a strong correlation between a characteristic metric representing per each limb, the limited knee extension of the patients and the effect of EMFT causing elevated spastic GRA forces.

The present findings, which show that in cerebral palsy, active state, rather than passive dominates the spastic muscle's joint movement limiting effect, and the effects of EMFT are a determinant of pathological gait, have clinical implications. One is for the clinical examination tests conducted prior to surgery. Ates et al. (2013b) studied muscle force-KA characteristics of individually activated spastic GRA intraoperatively and showed no correlation between the key determinants of the experimental measures (i.e., the KA and amplitude of peak spastic GRA force exertion, and the percentage of it measured at the most flexed and extended knee positions tested) and the outcome of patients' pre-operative clinical examinations performed in the passive state (a metric combining the popliteal angle and hip abduction angle into a clinical score for limited range of motion). The same general lack of active to passive state correlation was shown also for spastic ST (Ates et al., 2016) and semimembranosus (Yucesoy et al., 2017) muscles. Therefore, we suggest that clinicians pay a closer attention to a spastic muscle's impact on joint motion during active conditions as opposed the typical passive range of motion assessments conducted. Intraoperative clinical testing is ideally a tool to be used for that purpose, but this technique is not widely available currently. However, gait analyses should be central and the use of e.g., supersonic shear imaging is capable of estimating muscle force as well as EMFT effects (Ates et al., 2018; Yoshitake et al., 2018). Additionally, new approaches to interventions are warranted that consider the effect of agonist/antagonist interactions on a spastic muscle's limiting joint motion. Muscle related connective tissues also interconnecting those muscles are key to that. Tenotomy of spastic flexor carpi ulnaris was shown to be ineffective on wrist motion (Kreulen et al., 2003) and torque (de Bruin et al., 2011) unless accompanied with major dissection of the muscle's connective tissue envelope comprising epimuscular connections. Tendon transfer surgery involves partial dissection of connective tissues surrounding the muscle to be mobilized, which in return also interferes with the EMFT pathways (Yucesoy and Huijing, 2007). Muscle lengthening surgery directly interferes with muscular connective tissues: (i) intramuscularly, muscle's extracellular matrix is torn after the aponeurosis is transacted, which is determines the acute effects (Yucesoy et al., 2007). (ii) However, also epimuscularly, the preparatory dissections done to perform the main intervention can be effective and for the non-targeted muscles as well (Ates et al., 2013a). Those studies show that intra- and epimuscular connective tissues affect surgical outcome and the present study indicates they play a role in determining the spastic muscle's limiting joint motion. New studies should aim at determining if in CP, those connective tissues are stiffer so as to provide pathological agonist/antagonist connections. Also, possible effects of their altered structure and properties after the intervention should be accounted for to achieve optimal outcome.

Limitations of the work should be acknowledged. Fee and Miller (2004) showed in spastic CP, that active muscle tone disappeared under neuromotor blockade anesthesia, which was not used in the current study. Therefore, our findings may not have isolated pure passive state properties. However, this suggests that the spastic GRA's passive forces may be smaller than those reported. The maximum contraction condition used in intraoperative testing is unlikely to occur during gait. Moreover, the isometric condition does not represent the dynamic gait specific loadings. Therefore, the measured forces don't correspond directly to those acting on the joint during gait. However, the intraoperative data are important as the test conditions implemented allow for the quantification of the maximal capacity of the spastic GRA in limiting knee extension and the effects of added activation of other muscles on that. Note that, a similar effect of such co-activation also on proximal GRA forces is plausible, which may elevate its motion limiting effect at the hip, but this needs to be tested. New studies are indicated to consider different joint positions that represent other functional activities including altering of hip position into the coronal or transverse planes. Also testing of other medial hamstrings or plantar flexors is indicated for a broader understanding of mechanics of spastic muscle and effects of agonist/antagonist interaction on that.

5. Conclusion

Spastic muscle's passive forces measured directly for the first time in patients with CP maximally approximate a quarter of the active state forces, which attain peak values within the gait relevant KA-range and elevate significantly after the added activation of other muscles. Therefore, active state muscular mechanics, rather than passive, of spastic GRA present a capacity to limit joint movement in CP, the effects of which elevate due to intermuscular mechanical interactions.

Declaration of Competing Interest

The authors declare no conflict of interest.

Acknowledgements

We thank Uluç Pamuk, Agah Karakuzu and Orkun Akcan for their helps during intraoperative data collection, Shavkat Kuchimov for performing gait analyses of the patients, Utku Can for his helps in gait data processing, Rana N. Özdeşlik for the preparation of illustration and Emma Fortune for English editing. This work was supported by the Scientific and Technological Research Council of Turkey (TÜBİTAK) under grant 113S293 to Can A. Yucesoy. The study sponsors had no involvement in the study design in the collection, analysis and interpretation of data; in the writing of the manuscript; and in the decision to submit the manuscript for publication.

Appendix A. Pathological gait vs. effects of added activation of other muscles on spastic gracilis forces

Supplementary data to this article can be found online at https://doi.org/10.1016/j.clinbiomech.2019.06.005.

References

Ada, L., Vattanasilp, W., O'Dwyer, N.J., Crosbie, J., 1998. Does spasticity contribute to walking dysfunction after stroke? J. Neurol. Neurosurg. Psychiatry 64, 628–635. https://doi.org/10.1136/jnnp.64.5.628.

Arnold, A.S., Thelen, D.G., Schwartz, M.H., Anderson, F.C., Delp, S.L., 2007. Muscular coordination of knee motion during the terminal-swing phase of normal gait. J. Biomech. 40, 3314–3324. https://doi.org/10.1016/j.jbiomech.2007.05.006.

Ates, F., Özdeşlik, R.N., Huijing, P.A., Yucesoy, C.A., 2013a. Muscle lengthening surgery causes differential acute mechanical effects in both targeted and non-targeted synergistic muscles. J. Electromyogr. Kinesiol. 23, 1199–1205. https://doi.org/10.1016/j.jelekin.2013.05.010.

Ates, F., Temelli, Y., Yucesoy, C.A., 2013b. Human spastic Gracilis muscle isometric forces measured intraoperatively as a function of knee angle show no abnormal muscular mechanics. Clin. Biomech. 28, 48–54. https://doi.org/10.1016/j.clinbiomech.2012.08.012.

Ates, F., Temelli, Y., Yucesoy, C.A., 2014. Intraoperative experiments show relevance of

inter-antagonistic mechanical interaction for spastic muscle's contribution to joint movement disorder. Clin. Biomech. 29, 943–949. https://doi.org/10.1016/j.clinbiomech.2014.06.010.

Ates, F., Temelli, Y., Yucesoy, C.A., 2016. The mechanics of activated semitendinosus are not representative of the pathological knee joint condition of children with cerebral palsy. J. Electromyogr. Kinesiol. 28, 130–136. https://doi.org/10.1016/j.jelekin.2016.04.002.

Ates, F., Andrade, R.J., Freitas, S.R., Hug, F., Lacourpaille, L., Gross, R., Yucesoy, C.A., Nordez, A., 2018. Passive stiffness of monoarticular lower leg muscles is influenced by knee joint angle. Eur. J. Appl. Physiol. 118, 585–593. https://doi.org/10.1007/s00421-018-3798-y.

Crenna, P., 1998. Spasticity and "spastic" gait in children with cerebral palsy. Neurosci. Biobehav. Rev. 22, 571–578. https://doi.org/10.1016/S0149-7634(97)00046-8.

Damiano, D.L., Laws, E., Carmines, D.V., Abel, M.F., 2006. Relationship of spasticity to knee angular velocity and motion during gait in cerebral palsy. Gait Posture 23, 1–8. https://doi.org/10.1016/j.gaitpost.2004.10.007.

Davis, R.B., Õunpuu, S., Tyburski, D., Gage, J.R., 1991. A gait analysis data collection and reduction technique. Hum. Mov. Sci. 10, 575–587. https://doi.org/10.1016/0167-9457(91)90046-Z.

de Bruin, M., Smeulders, M.J.C., Kreulen, M., 2011. Flexor carpi ulnaris tenotomy alone does not eliminate its contribution to wrist torque. Clin. Biomech. 26, 725–728. https://doi.org/10.1016/j.clinbiomech.2011.03.007.

Farmer, S.E., James, M., 2001. Contractures in orthopaedic and neurological conditions: a review of causes and treatment. Disabil. Rehabil. 23, 549–558. https://doi.org/10.1080/09638280010029930.

Fee, J.W., Miller, F., 2004. The Leg Drop Pendulum Test performed under general anesthesia in spastic cerebral palsy. Dev. Med. Child Neurol. 46, 273–281.

Fergusson, D., Hutton, B., Drodge, A., 2007. The epidemiology of major joint contractures: a systematic review of the literature. Clin. Orthop. Relat. Res. 22–29. https://doi.org/10.1097/BLO.0b013e3180308456.

Gomez-Tames, J.D., Gonzalez, J., Yu, W., 2012. A simulation study: effect of the inter-electrode distance, electrode size and shape in transcutaneous electrical stimulation. In: Proceedings of the Annual International Conference of the IEEE Engineering in Medicine and Biology Society, EMBS, pp. 3576–3579. https://doi.org/10.1109/EMBC.2012.6346739.

Haberfehlner, H., Maas, H., Harlaar, J., Newsum, I.E., Becher, J.G., Buizer, A.I., Jaspers, R.T., 2015. Assessment of net knee moment-angle characteristics by instrumented hand-held dynamometry in children with spastic cerebral palsy and typically developing children. J. Neuroeng. Rehabil. 12. https://doi.org/10.1186/s12984-015-0056-y.

He, H., Kiguchi, K., Horikawa, E., 2007. A study on lower-limb muscle activities during daily lower-limb motions. Int. J. Bioelectromagn. 9, 79–84.

Huijing, P.A., Baan, G.C., 2001. Extramuscular myofascial force transmission within the rat anterior tibial compartment: proximo-distal differences in muscle force. Acta Physiol. Scand. 173, 297–311. https://doi.org/10.1046/j.1365-201X.2001.00911.x.

Huxley, A.F., Peachey, L.D., 1961. The maximum length for contraction in vertebrate striated muscle. J. Physiol. 156, 150–165. https://doi.org/10.1113/jphysiol.1961.sp006665.

Karakuzu, A., Pamuk, U., Ozturk, C., Acar, B., Yucesoy, C.A., 2017. Magnetic resonance and diffusion tensor imaging analyses indicate heterogeneous strains along human medial gastrocnemius fascicles caused by submaximal plantar-flexion activity. J. Biomech. 57, 69–78. https://doi.org/10.1016/j.jbiomech.2017.03.028.

Kreulen, M., Smeulders, M.J.C., 2008. Assessment of Flexor carpi ulnaris function for tendon transfer surgery. J. Biomech. 41, 2130–2135. https://doi.org/10.1016/j.jbiomech.2008.04.030.

Kreulen, M., Smeulders, M.J.C., Hage, J.J., Huijing, P.A., 2003. Biomechanical effects of dissecting flexor carpi ulnaris. J. Bone Joint Surg. Br. 85, 856–859. https://doi.org/10.1302/0301-620x.85b6.14071.

Lewerenz, A., Wolf, S.I., Dreher, T., Topcuoglu, M.S.Y., Krautwurst, B.K., 2017. Mechanisms to improve foot clearance while stair ascending in patients with bilateral spastic cerebral palsy and stiff knee gait. Gait Posture 57, 60–61. https://doi.org/10.1016/j.gaitpost.2017.06.289.

Maas, H., Baan, G.C., Huijing, P.A., Yucesoy, C.A., Koopman, B.H.F.J.M., Grootenboer, H.J., 2003. The relative position of EDL muscle affects the length of sarcomeres within muscle fibers: experimental results and finite-element modeling. J. Biomech. Eng. 125, 745–753. https://doi.org/10.1115/1.1615619.

Mathur, S., Eng, J.J., MacIntyre, D.L., 2005. Reliability of surface EMG during sustained contractions of the quadriceps. J. Electromyogr. Kinesiol. 15, 102–110. https://doi.org/10.1016/j.jelekin.2004.06.003.

Norton, B.J., Bomze, H.A., Sahrmann, S.A., Eliasson, S.G., 1975. Correlation between gait speed and spasticity at the knee. Phys. Ther. 55, 355–359. https://doi.org/10.1093/ptj/55.4.355.

Pamuk, U., Karakuzu, A., Ozturk, C., Acar, B., Yucesoy, C.A., 2016. Combined magnetic resonance and diffusion tensor imaging analyses provide a powerful tool for in vivo assessment of deformation along human muscle fibers. J. Mech. Behav. Biomed. Mater. 63, 207–219. https://doi.org/10.1016/j.jmbbm.2016.06.031.

Shortland, A.P., Harris, C.A., Gough, M., Robinson, R.O., 2002. Architecture of the medial gastrocnemius in children with spastic diplegia. Dev. Med. Child Neurol. 44, 158–163.

Smeulders, M.J.C., Kreulen, M., Hage, J.J., Huijing, P.A., van der Horst, C.M.A.M., 2004. Overstretching of sarcomeres may not cause cerebral palsy muscle contracture. J. Orthop. Res. 22, 1331–1335. https://doi.org/10.1016/j.orthres.2004.04.006.

Smith, L.R., Lee, K.S., Ward, S.R., Chambers, H.G., Lieber, R.L., 2011. Hamstring contractures in children with spastic cerebral palsy result from a stiffer extracellular matrix and increased in vivo sarcomere length. J. Physiol. 589, 2625–2639. https://doi.org/10.1113/jphysiol.2010.203364.

Van Heest, A.E., House, J.H., Cariello, C., 1999. Upper extremity surgical treatment of cerebral palsy. J. Hand Surg. Am. 24, 323–330. https://doi.org/10.1053/jhsu.1999.0323.

Willems, M.E.T., Huijing, P.A., 1994. Heterogeneity of mean sarcomere length in different fibres: effects on length range of active force production in rat muscle. Eur. J. Appl. Physiol. Occup. Physiol. 68, 489–496. https://doi.org/10.1007/BF00599518.

Yonetsu, R., Iwata, A., Surya, J., Unase, K., Shimizu, J., 2015. Sit-to-stand movement changes in preschool-aged children with spastic diplegia following one neurodevelopmental treatment session - a pilot study. Disabil. Rehabil. 37, 1643–1650. https://doi.org/10.3109/09638288.2014.972592.

Yoshitake, Y., Uchida, D., Hirata, K., Mayfield, D.L., Kanehisa, H., 2018. Mechanical interaction between neighboring muscles in human upper limb: evidence for epimuscular myofascial force transmission in humans. J. Biomech. 74, 150–155. https://doi.org/10.1016/j.jbiomech.2018.04.036.

Yucesoy, C.A., 2010. Epimuscular myofascial force transmission implies novel principles for muscular mechanics. Exerc. Sport Sci. Rev. 38, 128–134. https://doi.org/10.1097/JES.0b013e3181e372ef.

Yucesoy, C.A., Huijing, P.A., 2007. Substantial effects of epimuscular myofascial force transmission on muscular mechanics have major implications on spastic muscle and remedial surgery. J. Electromyogr. Kinesiol. 17, 664–679. https://doi.org/10.1016/j.jelekin.2007.02.008.

Yucesoy, C.A., Huijing, P.A., 2009. Assessment by finite element modeling indicates that surgical intramuscular aponeurotomy performed closer to the tendon enhances intended acute effects in extramuscularly connected muscle. J. Biomech. Eng. 131, 021012. https://doi.org/10.1115/1.3005156.

Yucesoy, C.A., Huijing, P.A., 2012. Specifically tailored use of the finite element method to study muscular mechanics within the context of fascial integrity: the linked fiber-matrix model. Int. J. Multiscale Comput. Eng. 10, 155–170. https://doi.org/10.1615/IntJMultCompEng.2011002356.

Yucesoy, C.A., Koopman, B.H.F.J.M., Grootenboer, H.J., Huijing, P.A., 2007. Finite element modeling of aponeurotomy: altered intramuscular myofascial force transmission yields complex sarcomere length distributions determining acute effects. Biomech. Model. Mechanobiol. 6, 227–243. https://doi.org/10.1007/s10237-006-0051-0.

Yucesoy, C.A., Ates, F., Akgun, U., Karahan, M., 2010. Measurement of human Gracilis muscle isometric forces as a function of knee angle, intraoperatively. J. Biomech. 43, 2665–2671. https://doi.org/10.1016/j.jbiomech.2010.06.002.

Yucesoy, C.A., Temelli, Y., Ates, F., 2017. Intra-operatively measured spastic semimembranosus forces of children with cerebral palsy. J. Electromyogr. Kinesiol. 36, 49–55. https://doi.org/10.1016/j.jelekin.2017.07.003.